

# **HOMOGENEOUS CHARGE COMBUSTION OF AQUEOUS ETHANOL**

---

**FINAL REPORT  
FEBRUARY 2001**

Report Budget Number KLK316  
Report N01-09

---

Prepared for

**RESEARCH AND SPECIAL PROGRAMS ADMINISTRATION  
U.S. DEPARTMENT OF TRANSPORTATION**

Prepared by

**NIATT**

**NATIONAL INSTITUTE FOR ADVANCED TRANSPORTATION TECHNOLOGY  
UNIVERSITY OF IDAHO**

Steven Beyerlein, Ph.D  
David McIlroy, Ph.D  
Donald Blackketter, Ph.D, P.E.  
Judi Steciak, Ph.D, P.E.  
Eric Clarke, Graduate Student  
Andron Morton, Graduate Student

## TABLE OF CONTENTS

<b>EXECUTIVE SUMMARY .....</b>	<b>1</b>
<b>DESCRIPTION OF PROBLEM .....</b>	<b>2</b>
<b>APPROACH AND METHODOLOGY .....</b>	<b>4</b>
Catalytic Igniter Concept .....	4
Aquanol Fuel.....	6
Surface Ignition Timing .....	7
Gas Phase Ignition Timing.....	8
Igniter Core Design.....	11
Engine Modifications .....	13
<b>FINDINGS; CONCLUSIONS; RECOMMENDATIONS .....</b>	<b>15</b>
Performance Data.....	15
Conclusions .....	21
Recommendations .....	22
<b>REFERENCES .....</b>	<b>23</b>

## **EXECUTIVE SUMMARY**

The goal of this research is to reduce nitrous oxide ( $\text{NO}_x$ ) and carbon monoxide (CO) emissions and to retain the performance characteristics of a diesel engine by modifying the in-cylinder combustion process. To accomplish this goal, a direct-injected diesel engine was converted to a homogeneous charge, catalytic compression ignition (HCCI). The engine runs on aqueous ethanol supplied by an electronic fuel injection system.

Central to this engine conversion is a catalytic igniter consisting of a platinum catalyst element enclosed in a small pre-chamber adjacent to the main combustion chamber. The catalytic igniter failed in initial tests with the high compression engine, forcing a redesign of the igniter core. Over 50 hours of engine testing were completed with the new igniter design. The testing was conducted with a mixture of 30 percent water and 70 percent ethanol. A tenfold decrease in nitrous oxide ( $\text{NO}_x$ ) emissions, a 10 percent increase in maximum power output, and a one percent improvement in specific fuel consumption were observed compared to the original engine configuration. Even more significant performance improvements are likely to occur in future engine testing when ignition timing is optimized. The results to date show promise for adding this technology to turbo-charged diesel engines.

## DESCRIPTION OF PROBLEM

Lean burning in piston engines affords a means of achieving important environmental and fuel economy objectives. To overcome the difficulties related to lean burning, Mark Cherry, president of Automotive Resources, Inc. (ARI), developed the Catalytic Plasma Torch (CPT) or SmartPlug™[1]. Several advantages of the SMARTPLUG design were noted over conventional spark ignition systems. These include increased power output, lower fuel consumption, extended lean-burn limits, reduced emissions, and simplified timing control [2, 3]. Despite its effectiveness as a tool for supporting lean combustion, SMARTPLUG technology has generated little interest in engine manufacturers or spark plug suppliers. This stems from waning interest in lean burn engines and recommitment to proven emissions after-treatment equipment. The primary drawbacks of lean burn engines are de-rated power output per unit displacement and incompatibility with oxidation/reduction catalysts used in conventional exhaust clean-up systems [4].

Over the last two years, the Sandpoint, Idaho, engine research company ARI has combined SMARTPLUG design with aqueous fuel technology to capture many of the benefits of lean burning without sacrificing power output. The aqueous fuel is a mixture of water, ethanol, and called Aquanol™ and is produced by Simplot Corporation, Caldwell, Idaho. Previous screening tests with portable electric generators, lawnmowers, rotary engines, and even diesel engines have indicated dramatic reductions in NO<sub>x</sub> and hydrocarbon emissions. Increases in thermal efficiency have also been noted. These improvements are sorely needed in small engine technology.

The National Institute for Advanced Transportation Technology (NIATT) at the University of Idaho is collaborating with Automotive Resources, Inc., to investigate long-term catalytic engine performance as well as catalyst durability. Various projects are underway with sponsorship from the Idaho Transportation Department (ITD), the Idaho Department of Water Resources (IDWR), the Idaho Space Grant Consortium (ISGC), and the US Department of Transportation University Transportation Centers Program. These include 200 hours of testing following the Engine Manufacturers Association (EMA) protocol with

periodic oil analysis and over-the-road testing of a converted spark-ignition transit van.

Future projects include over-the-road testing of a converted diesel truck and development of a pressurized flow reactor to study catalytic ignition phenomena.

## APPROACH AND METHODOLOGY

### Catalytic Igniter Concept

The SMARTPLUG is a self-contained ignition system that may be retrofitted to existing spark-ignition and compression-ignition engines. Key design features are illustrated in Fig. 1. The SMARTPLUG consists of a ceramic rod with an embedded heating element and a coating of noble metal catalyst. Cold starting requires up to 25 watts/igniter from an external power source (12 volt), which is no longer necessary after a few minutes of operation at idle. The catalytic core is enclosed in a custom-machined brass shell that forms a pre-chamber adjacent to the main combustion chamber. The shell fits into existing spark plug or direct fuel injection ports. The igniter used in this research has been made specifically for the direct injection ports on the 20-hp Yanmar engine.

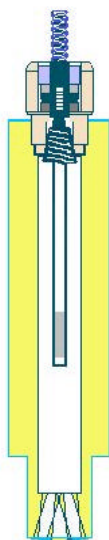


**Figure 1. SMARTPLUG Catalytic Igniter (US Pat. 5 109 817).**

Catalytic ignition in the SMARTPLUG begins as fresh mixture contacts the catalyst during the compression stroke. Because of the reduced activation energy associated with heterogeneous catalysis, this occurs at temperatures far below the normal gas-phase ignition temperature [5]. Combustion products and intermediate species then accumulate in the pre-

chamber surrounding the catalytic core. After sufficient temperature is achieved due to compression, multi-point homogeneous ignition results [5, 6]. The mixture is then rapidly expelled through the nozzles at the bottom of the igniter. The nozzles cause the flame torch to swirl and cover the entire combustion chamber in an exceedingly short period of time. The resulting flame pattern is illustrated in Fig. 2.

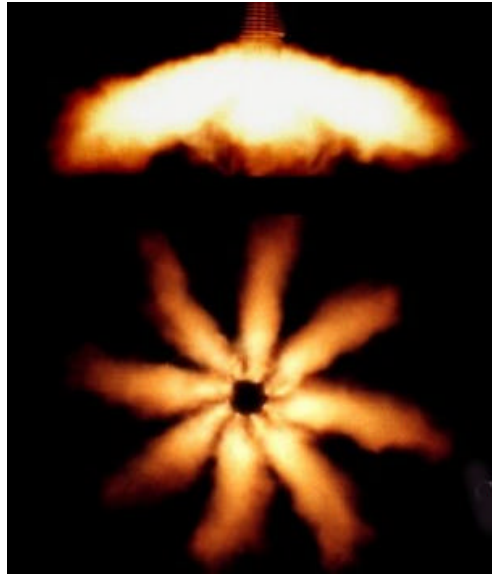


**Figure 2. SMARTPLUG flame pattern.**

Adjusting the location of the catalyst section on the ceramic rod controls ignition timing. To affect an ignition delay, the catalyst must be moved away from the nozzles at the bottom of the igniter. To affect an ignition advance, the catalyst probe must be moved closer to the nozzles. Use of SMARTPLUG technology allows the combustion of very lean fuel/air mixtures in the presence of water vapor [2].

The outer body of the igniter must be machined to match the combustion chamber opening. The internal volume of each igniter is about 7 percent of the original clearance volume. In the case of the Yanmar engine, addition of the pre-chamber volume to the top dead center volume reduced the compression ratio from 17.6 to 16.5. The internal diameter of the igniters is .25 in. and the four nozzles present a cross-section larger than the bore.

At present, the process of fabricating the internal parts of the igniter is labor intensive. Platinum wire must be precision wound onto the ceramic rod, and several miniature electrical connections must be made. In order for the igniter to seal properly, the ceramic rod must be bonded to a steel feed-through in a vacuum furnace. New designs are being investigated to eliminate many of these steps and to streamline the igniter production.

## **Aquanol Fuel**

Aquanol is environmentally friendly and more cost-effective than current alternative fuels . “Wet” alcohol fuels have much lower combustion temperatures than pure alcohol fuels or gasoline. This is the primary reason that aqueous fuels have such low  $\text{NO}_x$  emissions. The reduced temperatures also assure that catalytic materials are not degraded during the combustion process. This is important for extended life of the catalytic igniters.

Lowered combustion temperatures do not adversely affect engine efficiency. A MathCAD model of an idealized fuel-air-water cycle developed for this project illustrates that alcohol-water-air mixtures at a given equivalence ratio produce similar peak pressures to alcohol-air mixtures at the same equivalence ratio, even though the peak cycle temperatures are reduced by several hundred degrees. This means that due to the added mass of the water, specific work output is maintained while  $\text{NO}_x$  emissions are reduced to ultra-low emissions vehicle (ULEV) levels.

During the production of E-85 and E-95 fuel grade ethanol in the United States, the alcohol is distilled. It is then passed through a molecular sieve in order to reach 200 proof. Gasoline is then added as a denaturant. Aquanol, instead, will allow manufacturers to omit use of the molecular sieve—a costly and energy-intensive step. Stopping the distillation process at 140 proof would also greatly reduce the cost of the fuel. For this study, the pure alcohol was diluted with 35 percent water by volume. Bitrex, a commercial denaturant, and isopropyl alcohol was added instead of gasoline to meet federal regulations concerning denaturants.



Bitrix does not change the combustion characteristics of the fuel. Pure ethyl alcohol has a gross heating value of 29 MJ/Kg. When diluted to 35 percent water, the mixture has a gross heating value of 19 MJ/Kg. This compares with a heating value of 36 MJ/Kg for diesel fuel. Therefore to maintain a comparable energy input, it is necessary to modify the fuel delivery system to supply nearly twice as much Aquanol as diesel fuel.

Aquanol is environmentally friendly in another important way. Accidental spills biodegrade rapidly in comparison to petroleum-derived fuels, and expensive remediation of spill sites is avoided. For this reason, Aquanol is likely to become a preferred fuel for small watercraft.

### **Surface Ignition Timing**

Contact angle, and therefore surface ignition, is a function of igniter geometry and compression ratio. Catalytically-assisted ignition in internal combustion engines has two distinct phases. The first phase is catalytic oxidation of the fresh mixture entering the pre-chamber. Provided that the catalyst is above the surface ignition temperature for a given fuel, this begins as soon as the interface between the fresh charge and the residual gas from the previous cycle contacts the catalyst. The second phase is the auto-ignition of the unburned mixture that accumulates in the rear of the pre-chamber. Ideally, the second phase should have a finite and nearly constant duration for all engine-operating conditions. If this is the case, controlling the crank angle at which the fresh mixture contacts the catalyst can set ignition timing.

Since the pre-chamber length greatly exceeds the space between the ceramic rod and the igniter housing, diffusion between the fresh mixture and residual gas occurs slowly, and there is a well-defined interface between the fresh mixture and residual gas throughout the entire compression stroke. Because the nozzle area is approximately the same as the cross sectional area of the pre-chamber, gas dynamic effects during compression are negligible, and the compression ratio in the pre-chamber is the same as the compression ratio in the main chamber. Under these conditions the non-dimensionalized interface position  $x(\theta)/L_{pre}$  is a

function of piston, cylinder, and pre-chamber geometry. This quantity is a function of the non-dimensionalized piston location  $S_p(\theta)/L$  and the compression ratio  $r$ :

$$\frac{x(q)}{L_{pre}} = \frac{(1 - S_p(q)/L)}{(1 + 1/r)} \quad (1)$$

$$S_p(\theta) = (l_r + r_c) - \left[ \sqrt{l_r^2 - (r_c \cdot \sin(\theta))^2} + r_c \cdot \cos(\theta) \right] \quad (2)$$

In Eq. (1)  $x(\theta)$  is the interface position measured from the CPT nozzles,  $L_{pre}$  is the length of pre-chamber. In Eq. (2)  $S_p(\theta)$  represents the piston position measured from top dead center (TDC).  $L$  is the stroke,  $l_r$  is the connecting rod length, and  $r_c$  is the crank radius. Variables denoted  $(\theta)$  are a function of theta, which is the crank angle in degrees from TDC.

Figure 3 shows how  $x(\theta)/L_{pre}$  varies with crank angle for compression ratios of 9:1 and 16:1 in an engine with a bore/stroke ratio of unity. Notice that the interface location is almost identical for both compression ratios. The implication of this is that an igniter optimized for a single compression ratio can be fitted into engines with different compression ratios. This analysis assumes that the fuel composition, equivalence ratio and heat transfer remain unchanged. In previous low-compression engines, the catalyst was located at  $x/L_{pre}$  ratios between 0.3 and 0.4. This corresponds to a crank angle at first catalyst contact of more than 90 degrees before top dead center (BTDC). The Yanmar engine is considerably slower than previously studied spark ignition engines. As such, it would not be surprising if the ideal  $x/L_{pre}$  ratio for the catalyst was somewhat higher than 0.4. This corresponds to a shorter igniter core and less ignition advance.

## Gas Phase Ignition Timing

Gas phase ignition, unlike surface ignition, involves factors such as catalyst activity, catalyst reaction rates, densities of both fuel and air and charge energy content. As a first attempt to study gas-phase ignition delays associated with catalytic ignition, the igniter was divided into four zones for a lumped-parameter model. The four zones can be seen in Fig. 4. Each zone is characterized by a single temperature and fuel concentration. Pressure is constant across all

zones and is determined solely by piston displacement. Mass is progressively transferred from Zone I to Zone IV as the piston moves upward. The temperature and fuel concentrations in each zone are governed by equations of mass and energy conservation.

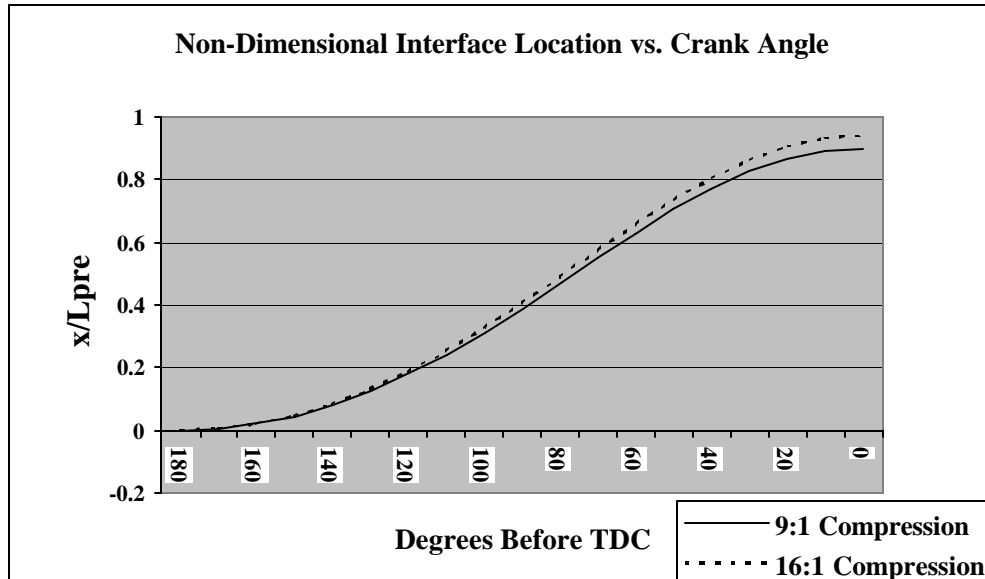


Figure 3. Interface location as a function of crank angle.

This model assumes that there is a clearly defined interface between the fresh air/fuel charge and combustion products from the last ignition event. During the compression stroke, the combustion products act like a gas spring. Zone I is the main chamber; Zone II is the region of the pre-chamber that does not surround the igniter core. Zone III is the region of the pre-chamber that surrounds the catalytic portion of the igniter core. This is the only zone

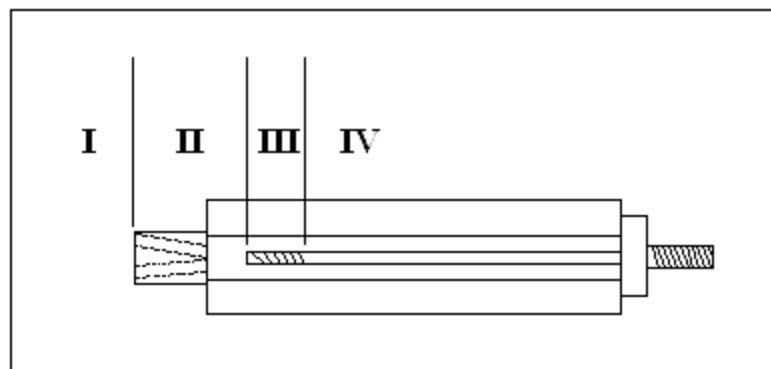


Figure 4. Igniter cutaway view with zones for ignition delay calculations.

where catalytic surface reactions take place. Also note that electrical heating is possible in this zone. Zone IV is the region of the pre-chamber that surrounds the non-catalytic portion of the igniter core. This is the only region where gas-phase reactions take place. Gas-phase ignition is assumed to occur when the gas-phase reaction rate exceeds the surface reaction rate.

It is assumed that reactions on the catalyst surface are mass transfer limited, while gas-phase reactions obey an Arrhenius relationship. Equation (3) is one of four simultaneous equations. The mass transfer terms are directly related to interface movement  $\frac{dx}{dt}$  which can be obtained from  $x(\theta)$  using the chain rule:

$$\dot{E}_{zone} = \left( \dot{q}_{het} + \dot{q}_{hom} - \dot{q}_{loss} \right) + \dot{m} h_{in} - \dot{m} h_{out} + \dot{W}_{comp} \quad (3)$$

In Eq. (3) the surface heat release rate  $\dot{q}_{het}$  is given by Eq. (4). This is a function of two reaction rates that are diffusion limited. Equation (4a) governs the diffusion of reactants and products to the catalytic surface. Equation (4b) is a competing reaction that blocks active catalyst sites with water molecules.

$$\dot{q}_{het} = r_1 - r_2 (HV)_{ethanol} \quad (4)$$

$$r_1 = \mathbf{r}_{ethanol} \mathbf{r}_{O_2} A_1 \quad (4a)$$

$$r_2 = \mathbf{r}_{H_2O} A_2 \quad (4b)$$

In Eq. (3)  $\dot{q}_{hom}$  is the gas-phase heat-release rate. Not only is this a function of reactant and product concentration, it is heavily dependant on temperature as shown in Eq. (5a).

$$\dot{q}_{hom} = r_3 (HV)_{ethanol} \quad (5)$$

$$r_3 = \mathbf{r}_{alcohol} \mathbf{r}_{O_2} A_3 \exp \left[ \frac{-E}{RT} \right] \quad (5a)$$

In Eq. (3)  $\dot{q}_{loss}$  accounts for thermal energy leaving the system via convection:

$$\dot{q}_{loss} = hA(T_{zone} - T_{wall}) \quad (6)$$

To integrate these equations,  $\dot{E}_{zone}$  takes the form of Eq. 7:

$$\dot{E} = C_v \frac{dT_{zone}}{dt} \quad (7)$$

In integrating these equations, time ( $t$ ) is explicitly linked to crank angle ( $\theta$ ). There will be an equation similar Eq. (3) for each of the four zones in Fig. 4. The solution will begin at the start of compression and will proceed until  $\dot{q}_{hom}$  exceeds  $\dot{q}_{het}$ . The crank angle where this occurs will be taken as the point of gas phase ignition. The difference between this angle and the contact angle can be defined as the ignition delay.

## Igniter Core Design

Igniter construction poses two major problems: Careful selection of materials that are compatible with the combustion environment and use of methods to streamline construction. The previous design was susceptible to destructive thermal cracking within a short period of use (10 minutes) and often took more than two days to construct. The new design consists of nine parts; all are shown in Fig. 5 except the platinum heating coil. These are assembled to form two main pieces, the electrical feed-through and the catalytic element. The feed-through consists of (from bottom to top in Fig. 5) a body, a pyrofolite washer, a terminal, an alumina washer, and a clamp that holds the terminal and washers in the body to form the gas tight seal. This portion of the igniter is universal and does not vary from engine to engine. The catalytic element consists of a custom alumina extrusion, a platinum heating coil (not shown), a threaded rod that connects the positive lead of the coil to the feed-through, and a conical spring that is used to connect the ground lead of the heating coil. The positive lead goes down the center of the alumina rod and then returns on the outside. A coating of plasma-sprayed alumina is applied over the rod to protect the coil from combustion temperatures, and then platinum paste is applied to the end over the heater. The platinum paste, once cured, serves as the catalytic ignition source. Changing the length of this catalytic

element is what controls ignition timing. Currently, new cores must be fabricated to explore different ignition timings.



**Figure 5. Improved CPT design.**

Finding sources of new materials has been just as important to igniter development as new fabrication techniques have been. The pyrofilite used in the feed-through is a compressible, machineable ceramic. Previous igniters did not use this material, so it was necessary to use an active metal braise (AMB) to form the gas tight seal. The AMB bonded the steel feed-through directly to the alumina rod. Because the process was delicate and lengthy, it would not be feasible for mass production. The AMB also alloyed with the platinum wire in the heating coil and made it extremely brittle. The failure rate of igniters employing the AMB was greater than 75 percent. Sealing defects were eliminated by substituting pyrofilite for AMB in the feed-through. Using a spot welder to attach the positive lead of the heating coil eliminated AMB embrittlement of the platinum wire.

The final hurdle to overcome in igniter construction was to develop a coating that would protect the platinum heating-coil. This coating needed to be approximately 0.010" thick and uniform in thickness. Several types have been tried, but the most promising is a plasma-

sprayed coating of alumina powder. This coating adheres well to the platinum heater wire, but not to the alumina rod at the center. The reason for this is the difference in the melting temperatures of the two materials.

## Engine Modifications

Table 1 shows the original specifications for the Yanmar diesel engine. Several modifications had to be made in order to make the engine compatible with Aquanol fuel. Because Aquanol is somewhat corrosive, stainless steel fuel injectors designed for E85 vehicles were mounted in the intake manifold and polypropylene fuel lines were installed. Removing the diesel fuel injectors yielded a suitable location for the catalytic igniters. With spark ignition engines, the igniters can be placed in the holes designed for the spark plug. A special research head is used with the Yanmar engine that contains an access port for an in-cylinder pressure sensor. A PCB model 12A piezoelectric transducer was selected for its reliability at high temperatures without requiring water-cooling. An optical encoder manufactured by Encoder Products was used to sense crankshaft position.

**Table 1. Yanmar Engine Specifications.**

Cylinders	3
Bore	7.49 cm
Stroke	7.49 cm
Displacement	998 cc
Compression Ratio	17.6:1
Rated Power	14.9 kW
Maximum Speed	3400 rpm

With instantaneous pressure and crank angle data available, igniter performance could be monitored and the igniter cores could be adjusted in and out for ideal ignition timing. During the first several hours of break-in when the engine ran on Aquanol, the engine burned an excessive amount of crankcase oil. This was traced to use of conventional piston rings. Conventional rings do not seal at the 150°F temperatures common to engines running on Aquanol. Total seal rings were chosen as more appropriate for this alternative fuels research

since they do not rely on thermal expansion to close the gap found in traditional piston rings. Installing total seal rings resolved the oil consumption problem.

Electronic fuel injectors supply fuel to the engine through the intake manifold. The injectors are pulse-width modulated to control fuel flow and are sized to accommodate the elevated flow rates, resulting from the lower energy content of the water fuel. The fuel injectors (Fig. 6) are controlled by a HalTech fuel computer.

The HalTech affords a means by which engine-fueling rates can be adjusted for various loading and operating conditions. Fuel maps can be downloaded from a PC to the HalTech. The fuel computer has several feedback sensors, such as a Hall-effect sensor, to pick up crank location and a throttle position sensor to provide engine speed control. Other sensors used by the HalTech system include an intake air thermocouple and an exhaust oxygen sensor. Unlike engines fueled with diesel or gasoline, an Aquanol-fueled engine can be over-fueled for increased power or run lean for increased fuel economy. This is due to the oxygen present in the fuel.



**Figure 6. Yanmar diesel engine intake manifold, fuel injectors (left side).**



## FINDINGS; CONCLUSIONS; RECOMMENDATIONS

### Performance Data

Figure 7 is a schematic of the experimental apparatus used for this work. Cylinder pressure and crank angle were the only computer-recorded data points. Engine speed, engine output, coolant temperature, exhaust temperature, emissions and fuel consumption were recorded by hand. A scale with 0.001-lb. resolution (not shown) was used to make five-minute fuel consumption measurements.

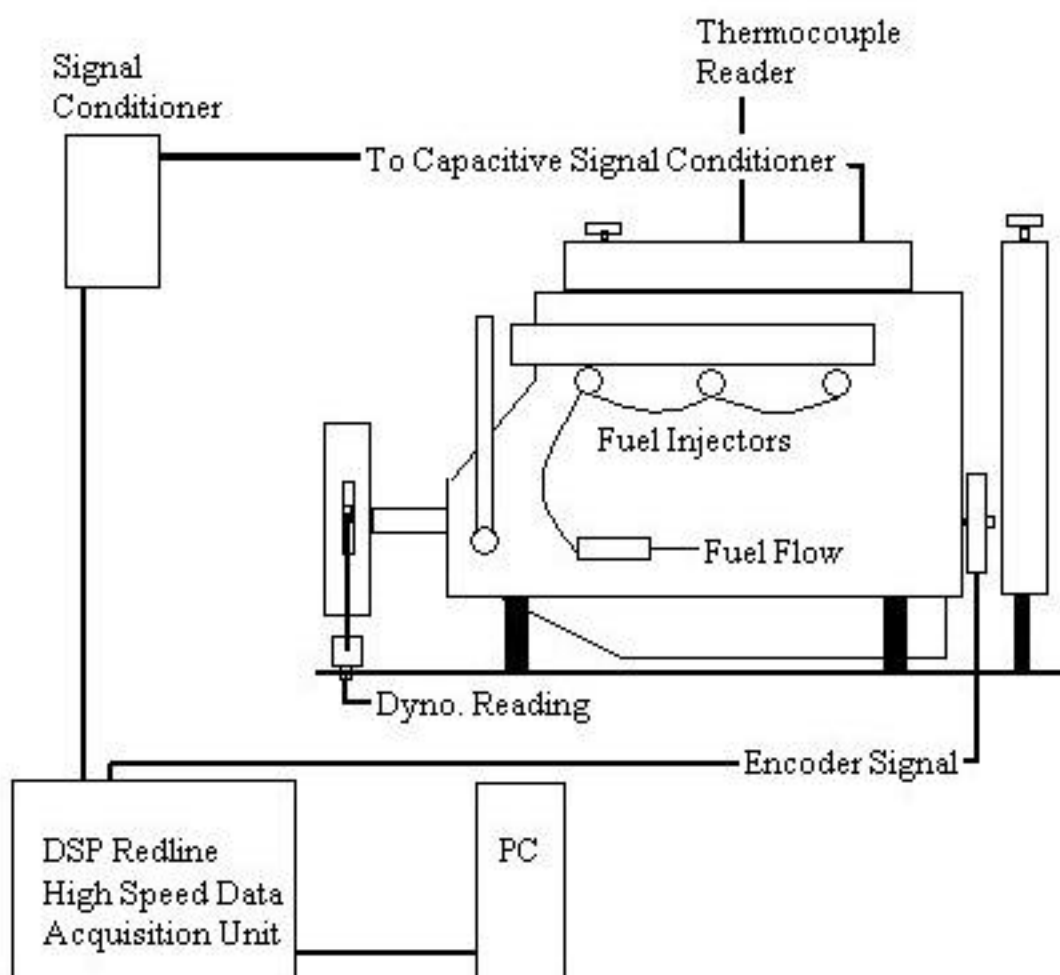
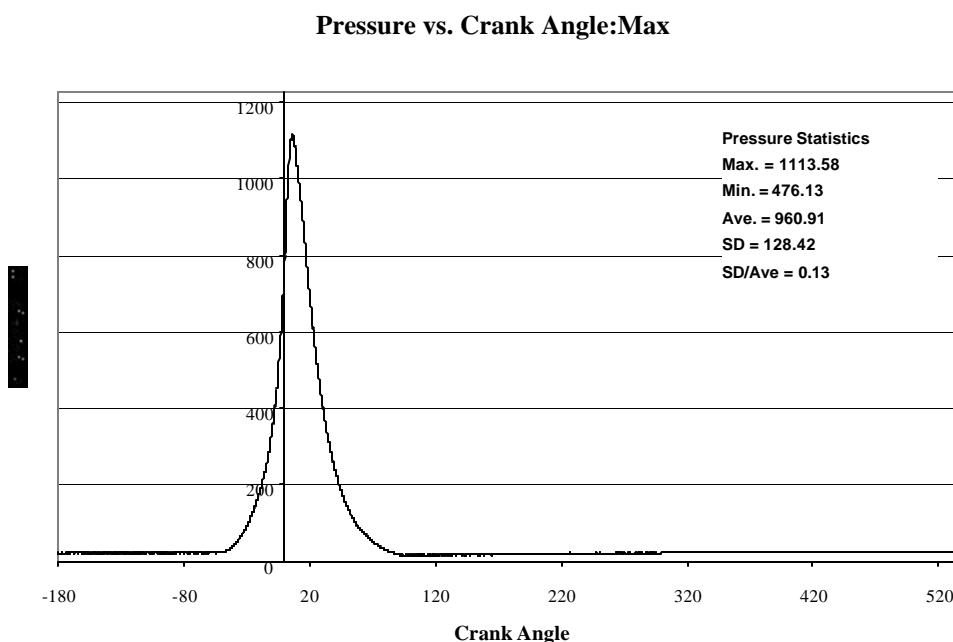


Figure 7. Experimental apparatus.

To gather instantaneous pressure data from the engine, a DSPT ACAP Redline data acquisition system was employed. A 333 MHz PC interfaces with the Redline system. ACAP Version 3 software controlled sampling and data storage. Inputs to the Redline equipment included exhaust and head temperature thermocouples, the crankshaft encoder, and the piezoelectric pressure transducer. A 90-hp Stuska water-brake dynamometer was used to measure steady state torque. In the set of tests reported here, engine output was limited to 40 percent of rated power.

ARI developed the Engine Cycle Analysis Tool (ECAT) software that was used to analyze the in-cylinder pressure data collected in this project. ECAT, a Visual Basic program, extracts data from the ACAP text file and decodes the ACAP output. The software calculates statistics on maximum pressure and indicated mean effective pressure (IMEP) and provides several options for visualizing pressure data.

Figures 8 through 11 are taken from ECAT analyses. Figure 8 shows pressure as a function of crank angle for a typical engine cycle at 2000 rpm and approximately 10 horse power.



**Figure 8. Pressure vs. Crank Angle,  $x/L_{pre}=0.63$ , 30 percent  $H_2O$ , 2000 rpm, 10-hp.**

Catalytic ignition begins 15 degrees before top dead center and maximum pressure is attained at 15 degrees after top dead center.

Figure 9 shows pressure as a function of volume for the same cycle. This profile is typical of an Otto cycle engine even though it is occurring in a homogeneous charge, compression-ignition engine. This is probably due to an increased air/fuel ratio at this operating speed. The fuel map for Aquanol in the Yanmar engine is still under development and it is likely that even better in-cylinder pressure statistics are possible after the map is optimized.

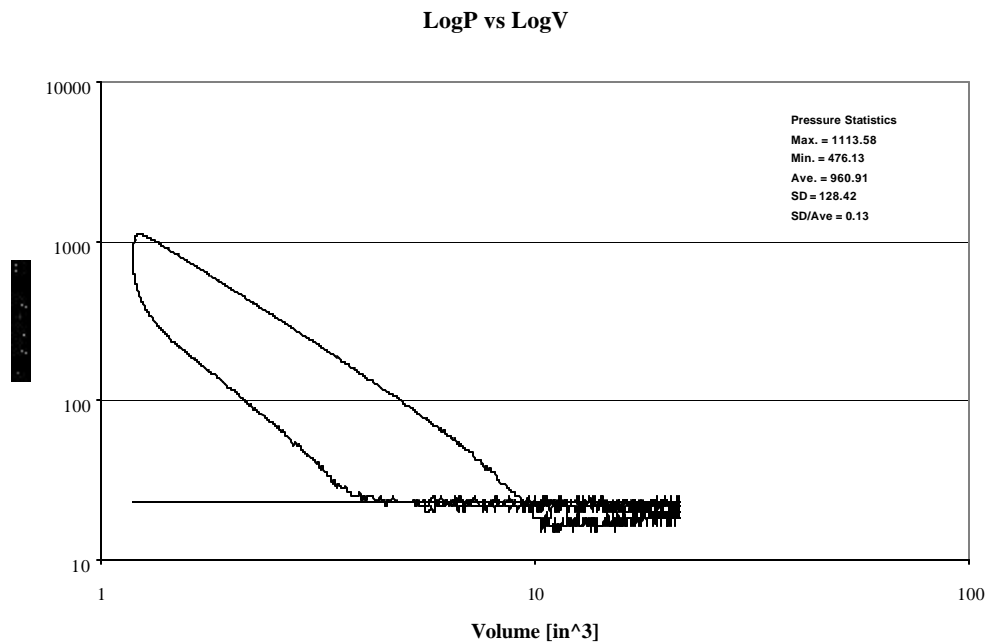


**Figure 9. LogP vs. LogV, x/Lpre=0.63, 30 percent H<sub>2</sub>O, 2000 rpm, 10-hp**

Proof that ignition timing is improved can be seen in Fig. 9. In this plot, there is little curvature at the beginning of combustion, indicating minimal heat release during compression. It has characteristic Otto Cycle shape. There was no audible detonation with 30 percent water content in the fuel. In addition to improved ignition timing, cycle-to-cycle pressure variation was vastly improved over standard length igniters. Figures 10 and 11 shows 50-cycle plots of pressure vs. crank angle that illustrates the improved repeatability of the pressure trace.

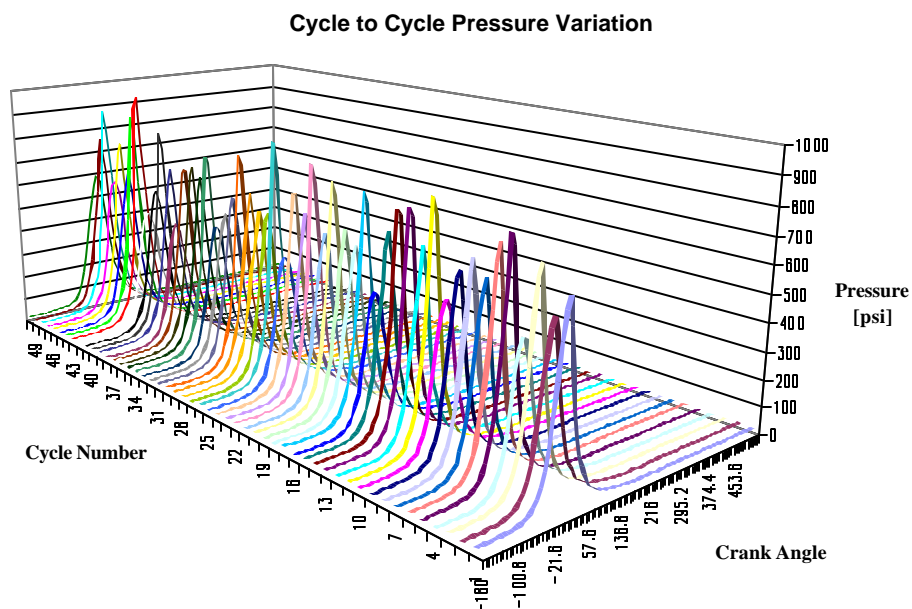


Figure 10. 50 Cycle pressure vs. crank angle traces for standard length igniters,  $x/L_{pre}=0.33$ , 30 percent  $H_2O$ , 1560 rpm, 8.73-hp.

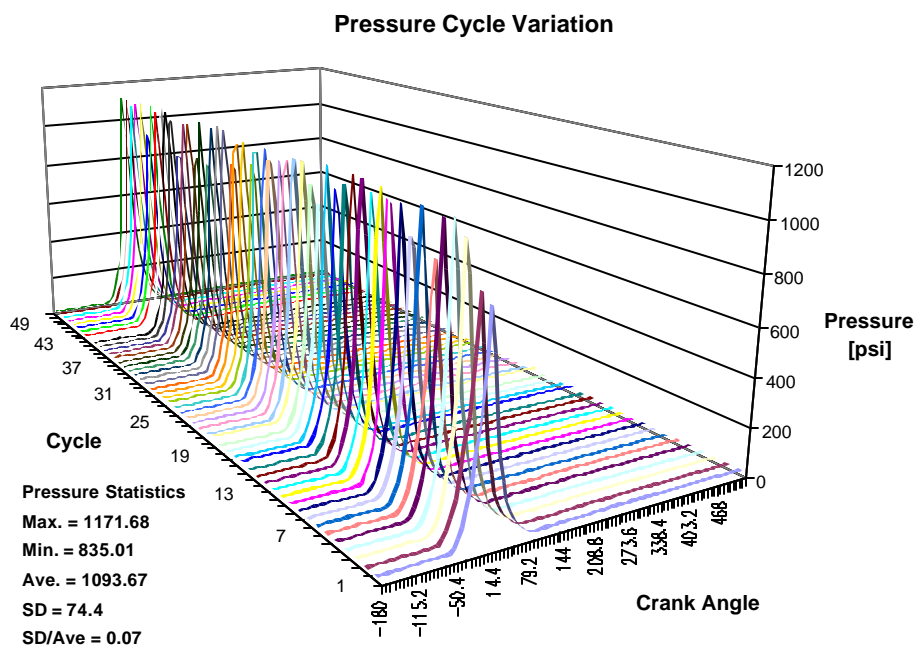


Figure 11. 50-Cycle pressure vs. crank angle traces for shorter igniters,  $x/L_{pre}=0.63$ , 30 percent  $H_2O$ , 2000 rpm, 10-hp.

Eight fuel consumption points were measured. Five of these were for 30 percent water. Table 2 contains brake specific fuel consumption (BSFC) data along with thermal efficiency and engine power output at five operating points. Specific fuel consumption is based on grams of pure ethanol, not grams of water/ethanol mixture. The addition of water beyond 30 percent eliminated detonation and allowed testing to continue but did not change ignition timing or affect fuel consumption.

**Table 2. Specific Fuel Consumption with 30 percent water/70 percent ethanol fuel.**

Specific Fuel Consumption [g/kW-h]	Thermal Efficiency [percent]	Power [kW]	Throttled
1103	17.6	3.14	yes
703	13.5	3.42	no
721	20	4.28	yes
769	19.5	4.45	yes
439	25.4	6.51	no

If ethanol and diesel fuels are considered on an equal-energy basis, the ethanol-burning engine should have a specific fuel consumption that is 62 percent higher. Figure 12 is a lugging curve based on the original diesel-burning configuration of the Yanmar engine.

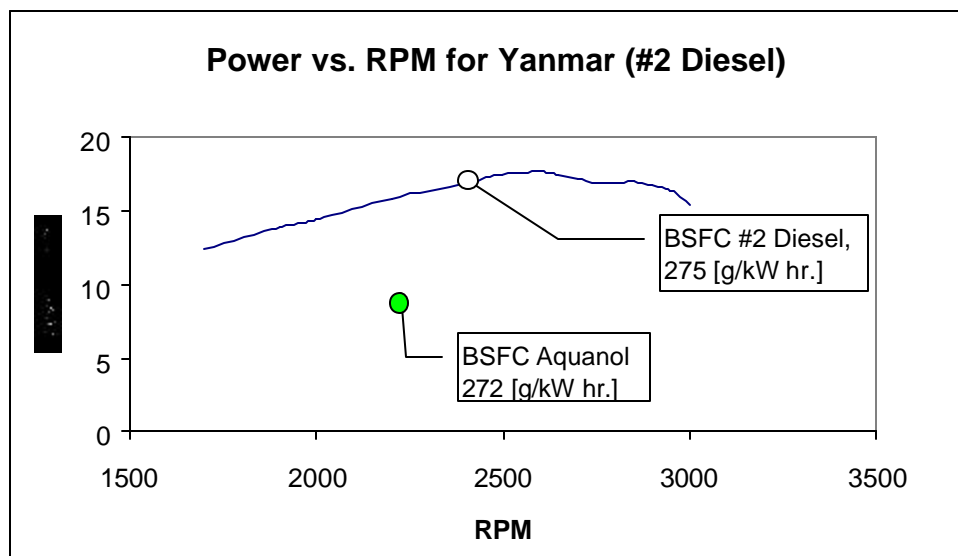


**Figure 12. Lugging curve with BSFC data points.**

Baseline specific fuel consumption for the Yanmar engine is 275 g/kW-hr (diesel). Because ethanol has only 62 percent of the energy content of diesel fuel, a corresponding fuel consumption value for ethanol is 443 g/kW-hr. The lowest value in Table 2 is 439 g/kW-hr (272 g/kW hr. diesel basis), which is 1 percent lower than the 443 g/kW-hr. benchmark. This small advantage is likely to grow larger when ignition timing and fuel mapping are optimized.

Table 3 contains emissions data at the five operating points reported in Table 2. Throttled vs. unthrottled operation appears to have a large impact on emissions. Under throttled conditions, CO and HC emissions were 18 percent higher than unthrottled operation. Emission values measured by the IR gas analyzer in parts-per-million.

**Table 3. Measured emission (sorted by power output), 30 percent H<sub>2</sub>O.**

CO [percent]	CO <sub>2</sub> [percent]	HC [ppm]	O <sub>2</sub> [percent]	NO <sub>x</sub> [ppm]	Power [kW]
0.35	10.2	1800	6.6	12	3.14
0.31	10.1	1513	7.2	10	4.28
0.36	10.2	1578	6.6	18	4.45
0.36	9.7	1900	6.8	25	6.51

In order to report this emission data on a brake specific basis, a MathCAD model was developed. The main assumptions behind this model were that the unburned hydrocarbons were in the form of methane, and NO<sub>x</sub> emissions were in the form of nitrogen oxide (NO). Fuel intake was experimentally measured, but intake air was not; therefore airflow was assumed to be a function of engine displacement and speed. Table 4 contains brake specific emissions data for operation on 30 percent water. Optimizing ignition timing and fuel mapping can reduce the values in Table 4.

**Table 4. Brake specific emissions (sorted by power output), 30 percent H<sub>2</sub>O.**

CO g/kW hr.	CO <sub>2</sub> g/kW hr.	HC g/kW hr.	NO g/kW hr.	Power [kW]
71.2	3261	20.9	0.331	3.14
53.4	2731	14.9	0.234	4.28
59.2	2636	14.8	0.402	4.45
36.9	1561	11.1	0.347	6.51

## Conclusions

Catalytically-assisted combustion of fuel-water mixtures represents a new paradigm for piston engine development. Instead of reducing pollutant emissions with after-treatment systems at the expense of engine power output, pollutant formation is controlled at the source by chemical and gas dynamic modification of the in-cylinder combustion process. The marriage of catalytic ignition with aqueous fuel technology allows engines originally designed for gasoline and diesel fuel to successfully run on alcohol. Although preliminary, this research with a direct-injected Yanmar engine has resulted in reduced NO<sub>x</sub> emissions and increased thermal efficiency as well as power output.

Other researchers have extensively described the dynamics of HCCI in a variety of engine types. This work illustrates how catalytic ignition expands the possibilities of HCCI. To better communicate these possibilities, a new acronym is suggested—homogenous charge catalytic compression ignition (HCCCI). Key elements of HCCCI include the following:

- Catalytic surface oxidation during the compression stroke at temperatures far below the normal gas phase ignition temperature,
- Accumulation of combustion products and active radicals in a small volume adjacent to the catalyst,
- Multi-point, compression ignition of gas mixture in the pre-chamber surrounding the catalyst near top dead center; and
- Rapid torch ignition of the fuel/air mixture in the main chamber.

## **Recommendations**

Future research on the Yanmar will include optimization of the igniter timing, engine oil analysis for water and other contaminants, characterization of igniter catalyst under extended operation, and engine durability testing. The robustness of the current igniter design will also be evaluated under higher temperature conditions expected in a turbo-charged direct injected (TDI) engine. Research on ignition limits of Aquanol fuel at different compression ratios would also be of value in planning future engine conversions. A study with a Cooperative Fuels Research (CFR) engine has been initiated to address this issue.



## REFERENCES

1. Cherry, M., Catalytic-Compression Timed Ignition, US Patent 5 109 817, December 18, 1990.
2. Cherry, M., R. Morrisset, and N. Beck, Extending Lean Limit with Mass-Timed Compression Ignition Using a Plasma Torch, Society of Automotive Engineers Paper #921556, 1992.
3. Gottschalk, Mark A., "Catalytic Ignition Replaces Spark Plugs," *Design News*, May 22, 1995.
4. Dale, J. and Oppenheim, A., A Rationale for Advances in Technology of IC Engines, Society of Automotive Engineers Paper #820047, 1982.
5. Cho, P. and C. Law, "Catalytic Ignition of Fuel/Oxygen/Nitrogen Mixtures over Platinum," *Combustion and Flame*, vol. 66, pp. 159-170, 1986.
6. Pfefferle, L., "Catalysis in Combustion, Catalysis Reviews," *Science and Engineering* vol. 29, pp. 219-267, 1987.
7. Thring, R., "Homogeneous-Charge Compression-Ignition (HCCI) Engines," Society of Automotive Engineers Paper #892068, 1989.